

## Lehigh University Lehigh Preserve

---

### Theses and Dissertations

---

2017

# Studying the role of cell competition in tumor progression via a two-dimensional vertex model

Bixi Kang  
*Lehigh University*

Follow this and additional works at: <https://preserve.lehigh.edu/etd>

 Part of the [Molecular, Cellular, and Tissue Engineering Commons](#)

---

### Recommended Citation

Kang, Bixi, "Studying the role of cell competition in tumor progression via a two-dimensional vertex model" (2017). *Theses and Dissertations*. 2948.

<https://preserve.lehigh.edu/etd/2948>

This Thesis is brought to you for free and open access by Lehigh Preserve. It has been accepted for inclusion in Theses and Dissertations by an authorized administrator of Lehigh Preserve. For more information, please contact [preserve@lehigh.edu](mailto:preserve@lehigh.edu).

Studying the role of cell competition in tumor  
progression via a two-dimensional vertex model

by

Bixi Kang

A Thesis

Presented to the Graduate and Research Committee

of Lehigh University

in Candidacy for the Degree of

Master of Science

in

Bio-engineering Program

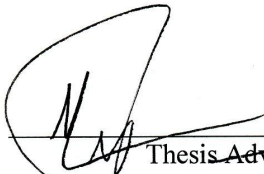
Lehigh University

(August 2017)

Copyright 2017, Bixi Kang

This thesis is accepted and approved in partial fulfillment of the requirements for the Master of Science.

6/30/17  
Date

  
Thesis Advisor

Anderson  
Chairperson of Department

  
\_\_\_\_\_

  
\_\_\_\_\_

  
\_\_\_\_\_

  
\_\_\_\_\_

# Contents

ABSTRACT:.....	- 2 -
1.Introduction.....	- 4 -
2. Methods.....	- 7 -
2.1 Vertex Model: Tissue Mechanics.....	- 7 -
2.2 Cell Cycle Dynamics: Tissue growth.....	- 10 -
2.3 Gene Regulation: Protein Dynamics.....	- 13 -
3. Results.....	- 17 -
3.1 A mathematical model predicts a critical size for tumor to overcome the apoptotic pressure from normal tissue in cell competition and expand.....	- 17 -
3.2 scrib-defective mutant cells are able to proliferate indefinitely.....	- 19 -
3.3 Oncogenic scrib- cells of the growing tumor are killed by JNK-mediated apoptosis when surrounded by wild-type cells.....	- 20 -
3.4 Tumor can overcome the apoptosis pressure exerted by the surrounding wild-type tissue and expand,with a large enough initial size ( 100 tumorous cells).....	- 21 -
3.5 Apoptotic rate of the tumorous cells are gained from the plotting of the dead cell numbers and it shows a positive correlation with the parameter $X$ .....	- 22 -
3.6 The simulation results fits well with the mathematical model in terms of the critical size of the initial tumor.....	- 23 -
4. Discussion:.....	- 24 -
References.....	- 26 -

## List of tables

Table 1. Values of parameters used in the simulation code (*TiFoSi*)

## List of figures

Figure 1: The vertex model for cell dynamics simulation.  $\alpha$  represents the individual cell sharing the vertex  $i$ ,  $j$  accounts for the vertices that share the vertex  $i$ , and  $l_{ij}$  represents the length of the edge connecting neighbor vertices  $i$  and  $j$ .

(Figure adapted from Reza Farhadifar et al., 2007, The Influence of Cell Mechanics, Cell-Cell Interactions, and Proliferation on Epithelial Packing)

Figure 2: T1, T2 and T3 transitions. T1 transitions are reversible but T2 and T3 are not. In a T1 process the recombination of cell neighbors is achieved by a cell edge that disappears and a new one that appears. T2 and T3 transitions are special cases of T1 transitions that involve triangular cells and lead to cell apoptosis/extrusion. T3 processes are extremely rare events under most conditions. In the figure the edges that undergo a transition are highlighted. (Figure adapted from TiFoSi Handbook V1.0, J.Buceta and O.Canela-Xandri.2014.)

Figure 3: The preferred cell apical area dynamics is divided into two phases, both of which last  $\tau/2$  in average. Given the value of the initial cell preferred area  $A_i$  and the final cell preferred area  $A_f$  for each phase, a linear piecewise dynamics is assumed. The blue line and the orange line describe individual tumor cell size dynamics and single normal cell area dynamics respectively. For both cell types, there is no growth at the first phase, but double the cell size at the second phase, while reaching the double size of cells' initial size, cell cleavage happens.

Figure 4: Cell competition involved proteins dynamics plotting. A. Protein *scrib* dynamics within different cell types and location. B. *JNK* dynamics within different cell types and location.

Figure 5: The progression of a tumor of size  $R$ , depends on two opposite effects: the apoptotic pressure (Blue arrows) from the surrounding normal tissue, exerted over the periphery cells, and the proliferating pressure (Green arrows) from the tumor bulk cells.  $d=2r$  being the characteristic cell diameter.

Figure 6: Exponential proliferation of compartments exclusively made of *scrib* mutant cells. A. *scrib* mutant cells exclusive compartment size changes over time. B. Plotting of the natural logarithm of *scrib* mutant cells number over the time. The slope represents the proliferation rate of the tumorous cells.

Figure 7: A. The alteration of the proportion of tumorous cells number over the initial tumorous cells number over time with different initial tumor sizes. B. Snapshots of the movie with 81 tumorous cells initially. The tumor disappeared gradually over time because of the apoptotic pressure from the normal tissue. Orange represents tumor group, purple stands for the normal tissue. C. Snapshots of the movie with 484 tumorous cells initially. The tumor overcome the apoptotic pressure from the normal tissue and expand. Blue accounts for the tumorous tissue and purple represents the normal tissue.

Figure 8: The positive correlation between the tumorous cells' apoptotic rate and the parameter  $X$ , which controls cells' contractility.

## ABSTRACT:

Tumor progression fate relies on the cell competition between tumorous cells and the surrounding regular cells. Studies on the *Drosophila* wing imaginal disc illustrate that cell competition can act either as a tumor suppressing or as a tumor promoting mechanism. However, how cell competition alters its role in tumor development via underlying molecular mechanisms as well as the role played by mechanical effects is still poorly understood. Here we study the role of cell competition in the early stage of tumor progression, using a simulation code of epithelial tissue (TiFoSi), which allows to include feedback between tissue growth, mechanics and gene regulation. Cells with inactivating mutations of tumor suppressor gene *scrib* always show hallmarks of carcinomas<sup>3,6</sup>. Multiple simulations show: 1) the clone of *scrib* mutant cells can be outcompeted and eliminated from the tissue, when surrounded by a wild-type tissue, even though they can proliferate infinitely on their own. 2) the initial size of the mutant clone can escape from the fate of elimination and expand, by protecting the inside cells from the range of cell competition, depending on the size of the initial tumorous clone. The results fits with experimental results and sheds light on how and why cell competition regulates tumor progression.

## KEY WORDS:

Cell competition, Apoptosis, *scrib*, *JNK*, Tumor

## 1.Introduction

Cancer can never be an outdated topic due to its prevalence all over the world and the limitation of current therapy methods. Over hundreds of years, numerous scientists and physicians were committed to researches about tumor and many great achievements have been made. However, there are still broad areas on the topics of tumor to be explored. In this context, recent studies propose that cell competition may play a critical role in tumor progression<sup>1,3,8,12</sup>, acting as either a tumor promoting mechanism or a tumor suppressing mechanism.

Cell competition is a homeostatic mechanism, in which cells with abnormal metabolic or behavior characteristics are identified and subsequently eliminated via Jun N-terminal Kinase (*JNK*) mediated apoptosis.<sup>3</sup> Cell competition can be initiated by the short-range cell-cell interaction between cells with different metabolism or behavior characteristics, which can be the result of a few genes' mutations. Cell competition was firstly described in the studying of *Drosophila* imaginal discs over 30 years ago.<sup>27,28</sup> The cells with heterozygous mutation of *Minute* gene were defeated by the surrounding wild-type tissue in the competition and subsequently eliminated by the programmed cell death (apoptosis), when mosaic flies containing these two types of cells were generated. However, the *Minute* heterozygous cells are viable on their own, suggesting the elimination of the mutant cells is attributed to the process of cell competition.<sup>8</sup>

Mutation of *dmyc* (*Drosophila* homologue of the proto-oncogene *MYC*), which promotes ribosome biogenesis, has also been shown to be able to induce cell competition between the mutants and wild-type cells. Similar as *Minute* mutants, clones carrying *dmyc* allele *dmyc*<sup>PO</sup>, showing a reduction of the *DMYC* function but not completely lost it, proliferate poorly when surrounded by wild-type cells and



are eliminated from the tissue, even though they are viable while in a homotypical environment<sup>8,20,27</sup>, which provides a further evidence that cell competition is in charge of the elimination of mutant cells.

Mutations in a series of tumor suppressing genes are also reported to trigger cell competition. These genes can be classified into two major groups, including *dlg1*, *lgl* and *scrib*, which are responsible for regulating cell polarity and proliferation<sup>3,12,18</sup>, as well as *TSG101*, *Vps25*, *Rab5* and *avalanche*, which are involved in the endosomal trafficking machinery.<sup>1</sup> Among these genes, *scrib* is the most studied in regards of cell competition. Cells with inactivating mutations of *scrib* typically hyperproliferate. However, when surrounded by wild-type cells, its proliferation advantage is compensated for by *JNK*-mediated apoptosis, as a result of cell competition, which is induced by the interaction with the outside wild-type tissue.<sup>3</sup> Evidence shows that the cell competition behavior is conserved in mammalian cells with mutant *scrib*.<sup>23</sup> This is a significant finding, since it shows evidence that when cell competition occurs among cells with different proliferation rates, it does not always lead to the elimination of slowly growing cells.

Recent studies suggest that there are two prerequisites for pre-oncogenic cells to survive and overgrow into tumors in the context of wild-type tissue. One is gaining a proliferate advantage over surrounding normal cells through a rescue signaling pathway, like *Ras* pathway. Another one is to form a microenvironment to protect cancerous cells inside clones from reaching the range of cell competition, by merging small tumor patches to form a large one.<sup>10,13,25</sup> That is, only cells at the tumor patch's periphery are eliminated via *JNK*-mediated apoptosis when surrounded by normal tissue. Moreover, it has been proposed that dying cells might release morphogen signals, like Decapentaplegic (*Dpp*), a *Drosophila* *BMP* homologue, to their neighbor cells to promote proliferation,

which is believed to act as a tumor promoting mechanism of cell competition.<sup>13,22</sup> The capability of mutant cells to overgrow and form a neoplastic tumor indeed depends greatly on the presence of apoptotic cells. Evidence shows that inhibiting apoptosis could lead to a significantly reduced proliferation of the mutants.<sup>15,21,22</sup> Besides, experimental observations have revealed that cells at the periphery that localized close to the apoptotic cells show high frequency of division activity.<sup>22</sup>

Mathematical modeling and computer simulation can be effective complementary tools to experiment approaches, which can provide a robust framework to better understand tumor progression. Currently emerging tissue modeling approaches can be classified into two major groups: the cell-based models and the continuous models. At the coarsest level, the tissue can be described as a continuous material (e.g. an incompressible viscous fluid). However, many cellular processes like cell migration, adhesion, cell polarity, directed division and differentiation cannot be described in a straightforward way by continuous models.<sup>28</sup> That is exactly why cell-based models are widely used for modeling of tumor growth, invasion and evolution in recent years. Current commonly used cell-based models includes Immersed Boundary Model, Subcellular Element Model, Cellular Potts Model, Vertex Model and Spheroid Model. All of Immersed Boundary Model, Subcellular Element Model and Cellular Potts Model have the problem of computational complexity. In comparison, Vertex Model and Spheroid Model are more computational efficient. But one critical issue with Spheroid Model is the omitted cellular details, like arbitrarily deformable shapes. In contrast, Vertex Model is not only relatively efficient, but also models explicit cell shapes allowing relatively high level of details. Accordingly, we applied a vertex model-based simulation code (*TiFoSi*), to study the cell competition's role in tumor progression in an epithelial tissue, which allows to include feedback between tissue growth, mechanics as well as gene regulation. The code relies on a text configuration file to design the computational

experiments and it generates different output files to save the data. We applied a visualization tool (*Wolfram Mathematica*) to process the data and generate movies.

In this thesis, we report a critical size of the *scrib* mutant clone, which is required for the mutant group to evade cell competition and overgrow into a tumor within an epithelial tissue, via running a series of simulations with different mutant clone's initial sizes. In our simulations, mutant cells situated at the clone periphery are killed by the *JNK*-mediated apoptosis and the proliferation rate of the cells close to the dead cells was improved via *Dpp* signals from the dying cells. The proliferation advantage of tumorous cells and normal cells in cell competition was compared. Statistically valid results were found after running the simulations with the same parameter setting for several times. Our observations validated the hypothesis that cell competition determines tumor's fate via the critical size threshold. This work provides a quantitative tool for the study of tumor progression and may be informative for the innovation of prospective tumor treatment methods.

## **2. Methods**

### **2.1 Vertex Model: Tissue Mechanics**

The vertex model, applied in the *TiFoSi* code for tissue dynamics implementation, was firstly proposed by Honda et al.<sup>14</sup> and was further adapted to epithelial tissues by some other authors.<sup>5,9</sup> It makes use of a series of vertices and the lines that connect neighbor vertices to form some enclosed polygons to represent the individual cell and the tightly pieced monolayer sheet of polygons to describe the entire tissue (see Fig. 1).

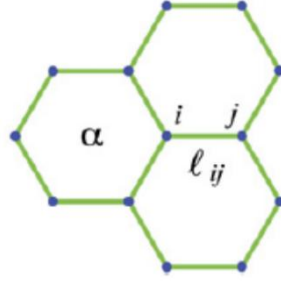


Figure 1: The vertex model for cell dynamics simulation.  $\alpha$  represents the individual cell sharing the vertex  $i$ ,  $j$  accounts for the vertices that share the vertex  $i$ , and  $l_{ij}$  represents the length of the edge connecting neighbor vertices  $i$  and  $j$ . (Figure adapted from Reza Farhadifar et al., 2007, The Influence of Cell Mechanics, Cell-Cell Interactions, and Proliferation on Epithelial Packing)

The energy functional (potential) acting on a cell vertex  $i$  in *TiFoSi* by the following function:

$$E(R_i) = \sum_{\alpha} \frac{K_{\alpha}}{2} (A_{\alpha} - A_{\alpha}^{(0)})^2 + \sum_{\langle i,j \rangle} \Lambda_{ij} l_{ij} + \sum_{\alpha} \frac{\Gamma_{\alpha}}{2} L_{\alpha}^2$$

Where the sums indexed by  $\alpha$  and  $\langle ij \rangle$  run respectively over the cells  $\alpha$  and vertices  $j$  sharing the vertex  $i$ . The terms on the right hand represent different energetic contributions. The first term stands for the elastic energy of cells and  $K_{\alpha}$  is proportional to the Young's Modulus, due to the difference between the actual cell area  $A_{\alpha}$  and the one  $A_{\alpha}^{(0)}$  that would have due to the cytoskeleton structure in the absence of the stresses associated with adhesion and cortical tension.<sup>17</sup> The term  $\Lambda_{ij}$  accounts for line tension, and  $l_{ij}$  represents the length of the edge shared by two neighbor cells, including the contributions from cell-cell adhesion as well as cortical tension, weighted by the parameter  $\Lambda_{ij}$ . The third term models the energetic contribution from the contraction of the actomyosin cortical ring, with  $\Gamma_{\alpha}$  being the contractile coefficient and  $L_{\alpha}$  representing the perimeter of the individual cell and takes into account a global contractility effect.<sup>17</sup>

We set elastic coefficient of tumor cells to be one order smaller than the normal cells' in the simulation experiments.<sup>16,26</sup> It has been reported that tumors tend to form a rounded clone while progressing to minimize their contact with the surrounding wild-type tissue, via increasing the interface boundary

junction tension.<sup>11</sup> Accordingly, we set the line tension of the edges located at the interface boundary to be significantly larger than that situated between the same type cells. We control the cortical ring contractility via *JNK* dynamics in the simulation. We set a threshold of *JNK* to determine whether the cortical contractility would be enhanced or not. When the amount of *JNK* are much higher than the threshold, there would be an extra value of parameter  $X$  contributing to the contractile level. Otherwise, the contractile levels are kept in a relatively low level with a constant value. In this way, we induced death of the cells that are with high levels of *JNK*, which are exactly the cells located at the tumor boundary.

By neglecting inertial effects with respect to dissipation, we consider an over-damped dynamics with a characteristic kinetic coefficient  $\gamma$ , assuming the total conservative force equilibrates with the dissipative force. Thus, the equation for the motion of vertex  $i$  at position  $r_i$

driven by the conservative force  $F_i = -\nabla E_i$  can be written as,

$$\gamma \dot{r}_i = F_i$$

The differential equations in *TiFoSi* are numerically integrated using an *Euler* algorithm.

As for the dimensions, we chose a reference cell type, “ $q$ ”, with properties  $K_q$  and  $A_q^0$  and the value of both  $\tilde{K}_q$  and  $\tilde{A}_q^0$  equals to 1. Accordingly, by choosing the following characteristic scales of length,  $l_c = \sqrt{A_q^0}$ , and time,  $t_c = \gamma / (K_q A_q^0)$ , the energy potential can be written in dimensionless form by defining the constants  $\tilde{K}_\alpha = K_\alpha / K_q$ ,  $\tilde{F} = F_\alpha / [K_q (A_q^0)^{3/2}]$ ,  $\tilde{\Lambda}_{ij} = \Lambda_{ij} / [K_q (A_q^0)^{3/2}]$  and  $\tilde{\Gamma}_\alpha = \Gamma_\alpha / (K_q A_q^0)$ . The characteristic values of the preferred tumorous cells’ area and normal cells’ area in dimensionless units reads  $\tilde{A}_{\alpha 1}^0 = A_{\alpha 1}^0 / A_q^0$  and  $\tilde{A}_{\alpha 2}^0 = A_{\alpha 2}^0 / A_q^0$  respectively.

Moreover, the simulation code includes a T1 recombination process and T2/T3 apoptosis /extrusion processes (see in Fig.2), which could alter the cell neighbor environment, to guarantee a biologically realistic evolution of the vertices connection network. All of the processes are triggered when

$$\tilde{l}_{ij} = 10^{-1} \tilde{l}^*, \text{ where } \tilde{l}^* = \sqrt{\frac{2}{3\sqrt{3}}}$$

is a characteristic edge size defined as the length of a regular hexagonal cell with area  $\tilde{A}_\alpha^0 |_{\alpha=q} = 1$ . Note that T1 is a reversible process, while both T2 and T3 processes are not reversible.

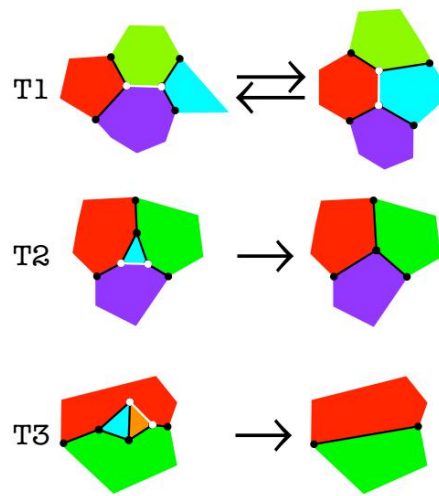


Figure 2: T1, T2 and T3 transitions. T1 transitions are reversible but T2 and T3 are not. In a T1 process the recombination of cell neighbors is achieved by a cell edge that disappears and a new one that appears. T2 and T3 transitions are special cases of T1 transitions that involve triangular cells and lead to cell apoptosis/extrusion. T3 processes are extremely rare events under most conditions. In the figure the edges that undergo a transition are highlighted. (Figure adapted from TiFoSi Handbook V1.0, J.Buceta and O.Canela-Xandri.2014.)

## 2.2 Cell Cycle Dynamics: Tissue growth

During the cell cycle duration, distinct growth phases are distinguished. We assume a simplified condition for the cell cycle description, dividing the cell cycle duration  $\tau$  into two phases, both of which last  $\tau/2$  in average. Within each phase the values  $A_i$  and  $A_f$  define the preferred cell apical area at the beginning and at the end of the phase. (dimensionless units, i.e. In units of  $\tilde{A}_q^0$ ). During the first

phase, cells do not grow and maintain their initial sizes  $\tilde{A}_\alpha^0$ . While, as long as the amount of time spend in phase I reaches  $\tau/2$ , and the actual apical area of the cell exceeds  $0.75 \tilde{A}_\alpha^0$ , cells enter the second phase and start to grow, increasing their size to double their initial preferred cell apical area  $A_\alpha^0$ , which is then followed by a cell division process. In addition, we set the tumor cells' size to be two times of the normal ones throughout the whole cell cycle duration in the simulation, due to experimental observations of giant polyploid cells in tumors.<sup>32</sup> (see Fig.3) A variable  $\tau$  representing the cell cycle duration was defined in the simulation approach as,

$$\tau = \varepsilon t_{\text{det}} + (1 - \varepsilon) t_{\text{sto}},$$

where  $t_{\text{det}}$  is a deterministic time scale representing a mean cell cycle duration in the absence of mechanical stress due to the cell local environment and  $t_{\text{sto}}$  is a random variable that stands for the variability of cell cycle duration and it is assumed to follow the following exponential distribution:

$$\rho(t_{\text{sto}}) = \frac{1}{t_{\text{det}}} e^{-\frac{t_{\text{sto}}}{t_{\text{det}}}}$$

The parameter  $\varepsilon$  controls the dispersion of the cell cycle duration. Accordingly, the average and standard deviation of  $\tau$  reads as the following respectively:

$$\langle \tau \rangle = t_{\text{det}}$$

$$\sigma_\tau = (1 - \varepsilon) t_{\text{det}}$$

$\langle \tau \rangle$  is the average cell cycle duration, which equals to  $1.6 \times 10^4$  in dimensionless units, which is around 22 hours in real time. Besides, the cell cycle duration is not deterministic but stochastic and depends on cell-autonomous processes and on the mechanical interactions with the cell local environment.

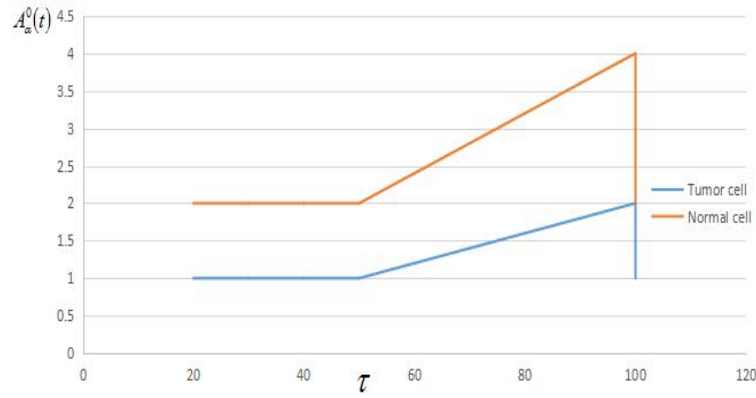


Figure 3: The preferred cell apical area dynamics is divided into two phases, both of which last  $\tau/2$  in average. Given the value of the initial cell preferred area  $A_i$  and the final cell preferred area  $A_f$  for each phase, a linear piecewise dynamics is assumed. The blue line and the orange line describe individual tumor cell size dynamics and single normal cell area dynamics respectively. For both cell types, there is no growth at the first phase, but double the cell size at the second phase, while reaching the double size of cells' initial size, cell cleavage happens.

Moreover, every time a cell divides, the clocks of daughter cells are reset and new random, putative cell cycle durations  $\tau$  are prescribed to each cell. The average cell cycle duration  $\langle \tau \rangle$  (dimensionless units, i.e. in units of  $t_c$ ) is determined by the cell growth rate (equals to 1) and the simulation time steps duration (equals to 0.01)<sup>18</sup> and equals to  $1.6 \times 10^4$  in the simulation.

It has been reported that *scrib* mutant cells show characteristics that overproliferate with high rates due to the constitutive expression of the *Ras* pathway.<sup>22</sup> But, since this work focuses mainly on the role of the tumor size, we disregarded the effect of proliferation rate and provided the same value of the cell growth rate for both tumorous cells and normal cells in the simulation to simplify the experiment.

As for the division orientation, the code evaluates the inertia tensor of the cell with respect to its center of mass. Upon the diagonalization of the inertia tensor we obtain the principle inertia axes and subsequently the longest axis of the cell (orthogonal to the direction along the largest principle inertia axis). The cells divide satisfying the *Hertwig* rule<sup>24</sup> such that the cleavage plane is perpendicular to the



longest axis and a random orientation is set by a Normal distribution around the putative division orientation.

### 2.3 Gene Regulation: Protein Dynamics

The dynamics of proteins suggested to be involved in cell competition during tumor progression is described in this part of the simulation by the following differential equation:

$$\frac{dP}{dt} = a \times A_{\alpha} - b \times P$$

where  $a \times A_{\alpha}$  stands for the initial production number of the protein  $P$ , and  $b$  represents the degradation rate of the protein, thus the second term accounts for the protein degradation. Obviously, the protein numbers would be equal to the value of the ratio  $\frac{a}{b}$  when it reaches the stationary state.

Based on the background section, the whole cell competition process can be mainly divided into three steps associated with different proteins: Firstly, *scrib* defective mutants initiates the cell competition with surrounding normal tissue; then the cells at the periphery of the tumor patch are induced to undergo apoptosis, which is regulated by *JNK*; finally, the apoptotic cells would send out the survival signals *Dpp* to their surrounding tissues to promote the cells' proliferation. We only described the first two procedure in the cell competition which involved *scrib*, *JNK* dynamics and also *Dpp* dynamics in our simulation, but did not include the compensatory proliferation procedure induced by capturing *Dpp* signals. We identified different production numbers ( $a_{Tscrib}$  and  $a_{Nscrib}$ ) of *scrib* for tumorous cells and normal cells, but the same degradation coefficient ( $b_{scrib}$ ) for both cell types, to set the different *scrib* level in tumor cells and normal cells after reaching the stationary state.(see in Fig.4A) Besides, we set different initial numbers of protein *scrib* in tumorous cells and normal cells.(see in Table 1)

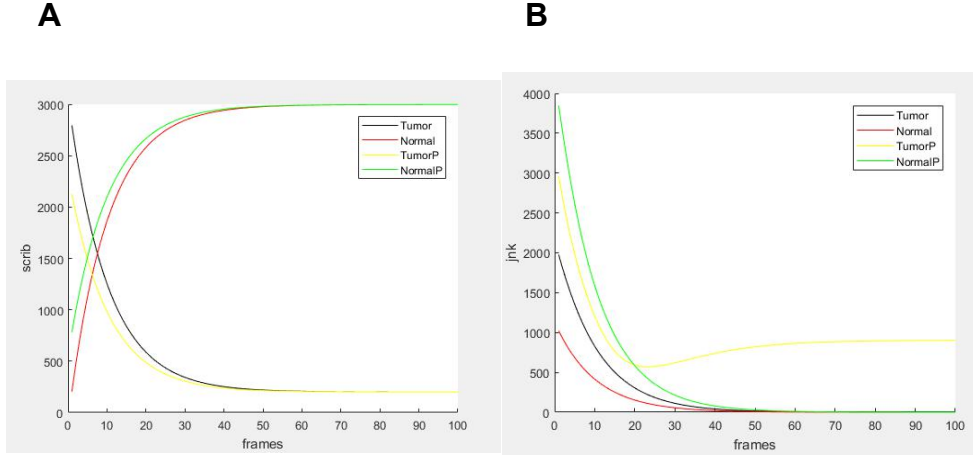


Figure 4: Cell competition involved proteins dynamics plotting. A. Protein *scrib* dynamics within different cell types and location. B. *JNK* dynamics within different cell types and location.

After that, we initiated *JNK* production driven by the different levels of *scrib* in tumorous cells and in normal cells. Firstly, each cell can sense the *scrib* levels from their neighboring cells. The precise mechanism is still unknown, but it has been implicated in several signaling pathways, such as vesicle trafficking. We quantified this neighbouring *scrib* levels by the following equation in our simulations,

$$scrib_{(sig)} = \sum_{ji} \frac{l_i}{L_i} scrib$$

where  $l_i$  represents the shared membrane (edge) with a neighbor cell and  $L_i$  accounts for the perimeters of the neighboring cells. The ratio of them accounts for the amount of *scrib* in each neighboring cell weighted. In addition, we identified the *scrib* level within each individual cell to be

$scrib_{(own)}$  in the simulation, which equals to  $\frac{a_{(scrib)}}{b_{(scrib)}}$  at the stationary state. Then we can easily get the

difference between  $scrib_{(sig)}$  and  $scrib_{(own)}$  ( $scrib_{(sig)} - scrib_{(own)}$ ).

For both tumor bulk cells and normal cells, the value of  $scrib_{(sig)} - scrib_{(own)}$  are close to 0, but for the cancerous cells situated at the tumor boundary, this value could be much larger. Accordingly, we

set a threshold  $T$  for the value of the difference  $scrib_{(sig)} - scrib_{(pro)}$ , to distinguish the tumorous cells located at the periphery from the tumor bulk cells and the normal cells by the equation,

$$f_1 = \begin{cases} 1, & \text{if } scrib_{(sig)} - scrib_{(pro)} > T / \tilde{A}_\alpha^0 \\ 0, & \text{if } scrib_{(sig)} - scrib_{(pro)} \leq T / \tilde{A}_\alpha^0 \end{cases}$$

We ran simulations with various values of the threshold  $T$  and found the value 745 of protein numbers is the most optimal value of  $T$  for our study, since it can not only ensure there is  $JNK$  signal only induced within the tumor boundary cells, but also make sure the boundary cells can be killed by the contractile pressure which is regulated via the  $JNK$  signal. Consequently, we incorporated the distinguished difference value into the differential equation for  $JNK$  dynamics to induce the production of  $JNK$  only within the tumorous cells located at the boundary,

$$\frac{dJNK}{dt} = a_{JNK} \times \frac{f_1 \times (scrib_{(sig)} - scrib_{(pro)})^4}{(200 / \tilde{A}_\alpha^0)^4 + f_1 \times (scrib_{(sig)} - scrib_{(pro)})^4} - b_{JNK} \times JNK$$

The value 200 here is a tested result as another threshold controlling  $JNK$  levels, which ensures  $JNK$  can be effectively activated within the tumor boundary cells and keep  $JNK$  levels low within tumor bulk cells and normal cells. (see in Fig.4B) It is worth noting that the initial number of  $JNK$  was set to be 0 for both cell types.(see in Table 1)

In the end, we figured out an equation to describe the dynamics of the survival signal  $Dpp$  in the apoptosis cells, whose production is induced by  $JNK$  :

$$\frac{dDpp}{dt} = a_{Dpp} \times \frac{JNK^4}{1500^4 + JNK^4} \times \tilde{A}_\alpha^0 - b_{Dpp} \times Dpp + D \times \nabla^2 Dpp$$

where  $D$  accounts for efficient diffusion coefficient (dimensionless units)<sup>2</sup> and  $\nabla^2 P$  stands for diffusion operator ( more details see in TiFoSi: an Efficient Simulation Suit for Epithelia).<sup>18</sup> In this way,  $Dpp$  is induced in the dying cells and it sends out the signal through a formation of the concentration gradient. However, the underlying mechanism of inducing  $Dpp$  signals and how  $Dpp$  functions to promote tumor

proliferation is still an open question. Thus, we did not include *Dpp* relative dynamics in our simulation tests.

The total simulation time is  $8 \times 10^4$  in dimensionless units, which is around 111 hours in real time.

There is 200 frames in total and the time between frames is 400 in dimensionless units, which is approximately 33 minutes in real time units. We have three parameters involved:  $\Delta$  represents time steps, equals to 0.01 in dimensionless units;  $M$  indicates the number of simulation blocks with a size  $P$ , and  $P$  stands for the number of time steps of each of the blocks. Thus, the total duration of the simulation in dimensionless time units is,

$$M \times P \times \text{deltat}$$

(All of the parameter values used in the simulation see in Table 1.)

Table 1. Values of parameters used in the simulation code (TiFoSi)

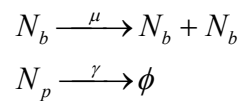
	$K_\alpha$ (16,25)	$\Lambda_{ij}$ (11)	$\Gamma_\alpha^{(13)}$	$a_{scrib}$	$b_{scrib}$	$scrib$	$a_{JNK}$	$b_{JNK}$	$JNK$	$a_{Dpp}$	$b_{Dpp}$	$D$	$M$	$P$	$\Delta$
Tumor cells	0.25	0.01	$0.005 \times (1 + 15 \times \begin{cases} 0 & \text{if } jnk < 1000A \\ 1 & \text{if } jnk > 1000A \end{cases})$	0.056	$2.78 \times 10^{-4}$	0	0.55	$2.78 \times 10^{-4}$	0	$4 \times 10^3$	$1.25 \times 10^{-3}$	$5 \times 10^{-3}$	200	$4 \times 10^4$	0.01
Normal cells	2.5	0.01	0.01	0.833	$2.78 \times 10^{-4}$	0	0.55	$2.78 \times 10^{-4}$	0	$4 \times 10^3$	$1.25 \times 10^{-3}$	$5 \times 10^{-3}$	200	$4 \times 10^4$	0.01
Between	-	0.06	-	-	-	-	-	-	-	-	-	-	-	-	-

### 3. Results

#### 3.1 A mathematical model predicts a critical size for tumor to overcome the apoptotic pressure from normal tissue in cell competition and expand.

Based on the “microenvironment theory” mentioned above, we proposed a simplified math model to predict the growing dynamics of neoplastic tumors. Our calculation result shows that only if the tumor size reaches a critical value, it can survive and develop. Otherwise, the tumor would be cleared out due to the apoptotic pressure from surrounding normal tissues. Our result shows a good compatibility with the “microenvironment theory”.

We considered a tumor that is composed of  $N$  cancerous cells, which are composed of two parts, the bulk of the tumor with  $N_b$  cells and the periphery of the tumor with  $N_p$  cells (see Fig.5). That is,  $N = N_b + N_p$ . Then we assume a simplified situation for tumor progression with cell proliferation at the tumor bulk at a rate  $\mu = \ln(2)/\tau$  ( $\tau$  being the average cell cycle duration) and cell apoptosis at the tumor’s periphery at a rate  $\gamma$ . These two processes can then be expressed as following reactions:



Then we can easily reach the following differential equation for the number of cells in the tumor:

$$\frac{dN}{dt} = \mu N_b - \gamma N_p$$

On the other hand, we assume that neoplastic tumors display a characteristic circular geometry, and we define the characteristic cell radius as  $r = \sqrt{\langle A \rangle / \pi}$ , where  $\langle A \rangle$  is the average cell area. Thereby, we can relate the number of tumor cells  $N$  with the tumor radius  $R$  by the following equation:

$$\pi R^2 = N \langle A \rangle$$

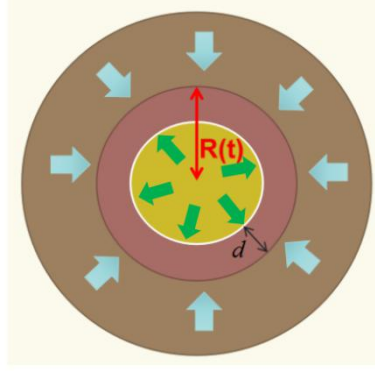


Figure 5: The progression of a tumor of size  $R$ , depends on two opposite effects: the apoptotic pressure (Blue arrows) from the surrounding normal tissue, exerted over the periphery cells, and the proliferating pressure (Green arrows) from the tumor bulk cells.  $d=2r$  being the characteristic cell diameter.

Thus,

$$N = \left( \frac{R}{r} \right)^2$$

Accordingly, the number of cells in the tumor bulk and at the tumor periphery satisfy the following equations (assuming  $R \gg r$ ):

$$N_b = \frac{\pi (R - 2r)^2}{\pi r^2} = \left( \frac{R}{r} \right)^2 - 4 \left( \frac{R}{r} \right) + 4 \approx \frac{R}{r} \left[ \left( \frac{R}{r} \right) - 4 \right]$$

$$N_p = \frac{\pi R^2 - \pi (R - r)^2}{\pi r^2} = \frac{4Rr - 4r^2}{r^2} \approx 4 \frac{R}{r}$$

Consequently, the radius  $R$  of the tumor satisfies the following differentiation equation:

$$\frac{1}{r} \cdot \frac{dR}{dt} = \frac{\mu}{2} \left[ \left( \frac{R}{r} \right) - 4 \right] - 2\gamma$$

Then by defining  $z = R/r$  (the radius of the tumor in units of the characteristic cell radius) and

$\tilde{t} = \mu t$  (time in units of proliferation rate), we finally obtain the dimensionless equation:

$$\frac{dz}{d\tilde{t}} = \frac{z}{2} - 2(1 + \lambda) \quad (1)$$

where  $\lambda = \gamma/\mu$ . And the solution to equation (1) reads:

$$z(t) = z_c + e^{\frac{\tilde{t}}{2}} [z_0 - z_c]$$

where  $z_0 = R(t_0)/r$  and  $z_c = 4(\lambda + 1)$ , being the initial radius of the tumor clone in units of the

characteristic cell radius and the critical value of the tumor radius respectively.

According to the analytic calculations above, we can easily reach the prediction that if  $z_0 > z_c$ , which means the initial size of tumor is larger than the critical size, the tumor would overcome the apoptotic pressure exerted from the surrounding normal tissue and expand, increasing its radius exponentially.

While, if  $z_0 < z_c$ , the apoptotic pressure will finally clear out the tumor. It is also worth noting that the

critical radius increases linearly as a function of  $\lambda = \gamma/\mu$ , the ratio of the reproduction rate of the tumor bulk cells over the apoptotic rate of the tumor periphery cells. Moreover, if the whole tissue has a

typical size  $\rho$  (the tissue radius in units of the characteristic cell radius), then the maximum number of the tumor patches with initial size  $z_0$  that can fit in the tissue without overlaying should be  $n_c = (\rho/z_0)^2$ .

Consequently, if  $n > n_c$ , some patches would merge, leading to a larger size of the tumor patch. That

is, even if the initial individual size of some patches is smaller than the critical tumor size, they can still survive and grow finally due to the coalescence, which can lead them to an effective initial size to

overcome the apoptotic pressure from outside. Finally, if  $z_c > \rho$ , then it is obvious that  $z_c > z_0$ .

Namely, if the critical tumor size is larger than the whole tissue size, then certainly it is larger than the initial size of the tumor patch, the tumor would be annihilated by the apoptotic pressure for sure. This

sets a condition for the apoptotic rate that ensures tumor annihilation,

$$\gamma \leq \mu \left( \frac{\rho}{z_0} - 1 \right)$$

### **3.2 scrib-defective mutant cells are able to proliferate indefinitely.**

Firstly, we run a series of simulations with only one cell type, the *scrib* defective mutant cells, starting with an initial size of 36 cells, in various simulation times. The mutant cells keep proliferating and

expanding over the time, even in the simulation with the maximum simulation times that simulates

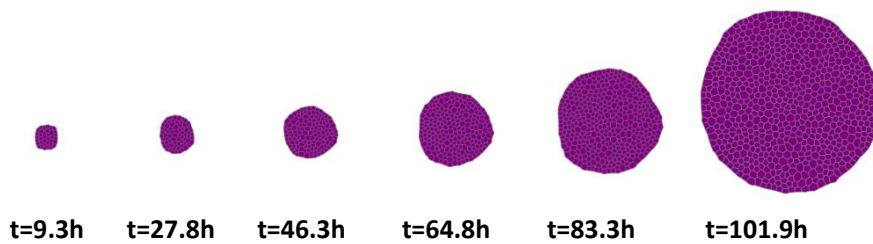
tissue growing over 111 hours, which suggests that compartments exclusively made of *scrib* mutant

cells are capable to proliferate indefinitely. (see in Fig.6A) Normal tissues behaved just as the same and the relative data is omitted. Assuming the mutant cells are proliferating exponentially, that satisfies the following function,

$$N = N_0 e^{\lambda t}$$

Then the slope in the plotting for the natural logarithm of the mutant cell numbers over time should stand for the proliferation rate of the tumorous cells. (see in Fig.6B)

**A**



**B**

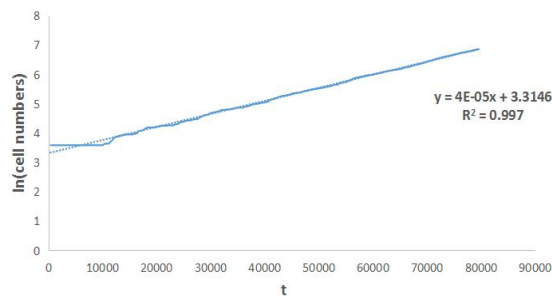


Figure 6: Exponential proliferation of compartments exclusively made of *scrib* mutant cells. A. *scrib* mutant cells exclusive compartment size changes over time. B. Plotting of the natural logarithm of *scrib* mutant cells number over the time. The slope represents the proliferation rate of the tumorous cells.

### 3.3 Oncogenic *scrib*- cells of the growing tumor are killed by JNK-mediated apoptosis when surrounded by wild-type cells.

We run some simulations with both cell types involved, and make the *scrib* mutant tumorous cells surrounded by the normal cells. We started with a simulation that has a relatively small initial tumor size (25 cell) within a 400-cell normal tissue. Via adjusting the value of the parameter  $X$ , which

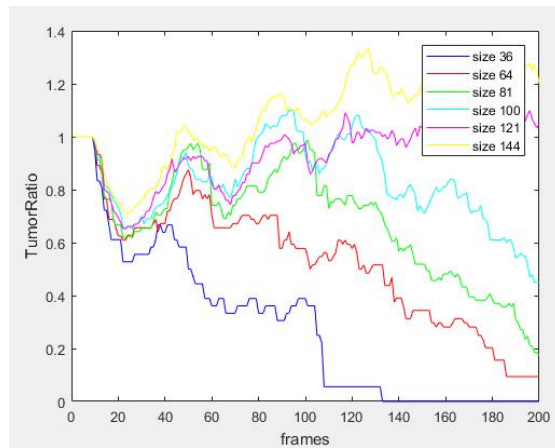


controls the level of the contractile strength depending on *JNK* levels (with a high enough *JNK* level, this parameter would be multiplied into the small value of the contractile parameter  $\Gamma_{\alpha}$  to increase the contractile pressure, otherwise, the small value of the contractile parameter  $\Gamma_{\alpha}$  would not change), we found that when  $X = 15$ , all of the tumorous cells are eliminated within the simulation time.

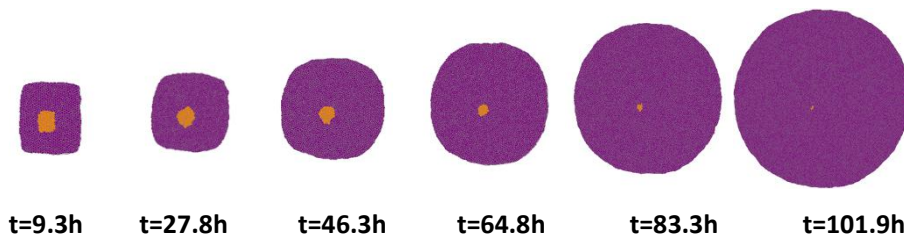
### **3.4 Tumor can overcome the apoptosis pressure exerted by the surrounding wild-type tissue and expand, with a large enough initial size ( 121 tumorous cells).**

We then run simulations remaining  $X = 15$ , but with various initial tumor sizes (36 tumorous cells, 64 tumorous cells, 81 tumorous cells, 100 tumorous cells, 121 tumorous cells, 144 tumorous cells, all within a 900-cells normal tissue), to test the viability of the critical size hypothesis. The simulation results show that tumor can evade from the fate being eliminated by the surrounding normal tissue, proliferate and expand, with a 121-cells initial size. Otherwise, if the initial tumor size is smaller than 121 mutant cells' size within a normal tissue with 900 cells, it is outcompeted by normal cells via *JNK*-mediated apoptosis. (see in Fig.7) Accordingly, we got the critical size for tumor development with the presence of cell competition against surrounding normal tissues, which is around the size of 121 tumorous cells. Similar experiment observation has been reported for *Rab5<sup>KD</sup>* tumor, which is capable of surviving and growing with a critical size of 400 cells. <sup>2</sup> The slight difference between the simulation results and previous experiment observation may be caused by the overestimated contractility level in our simulation.

**A**



**B**



**C**

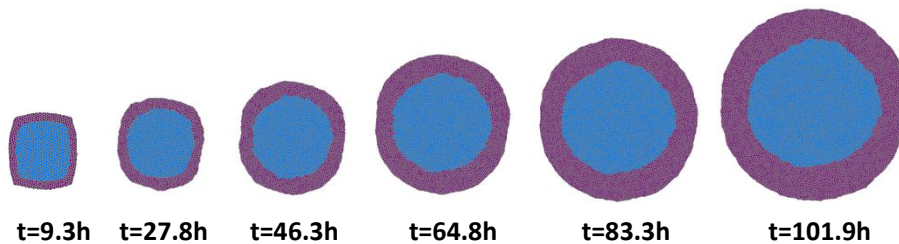


Figure 7: A.The alteration of the proportion of tumorous cells number over the initial tumorous cells number over time with different initial tumor sizes. B.Snapshots of the movie with 81 tumorous cells initially. The tumor disappeared gradually over time because of the apoptotic pressure from the normal tissue. Orange represents tumor group, purple stands for the normal tissue. C.Snapshots of the movie with 484 tumorous cells initially. The tumor overcome the apoptotic pressure from the normal tissue and expand. Blue accounts for the tumorous tissue and purple represents the normal tissue.

### 3.5 Apoptotic rate of the tumorous cells are gained from the plotting of the dead cell numbers versus time and it shows a positive correlation with the parameter $X$ .

We run a series of simulations with different values of the parameter  $X$  and plotted the dead cell numbers versus time, assuming that cells died linearly, even though the linear fitting showed some noises. Then we got the apoptotic rate correlated with each parameter  $X$  value from the slope of the plotting and then plotted the relation between the parameter  $X$  and the apoptotic rate. We found that

apoptotic rate is positively correlated with the parameter  $X$ , which means we can adjust apoptotic pressure via adjusting the value of the parameter  $X$ . (see in Fig.8)

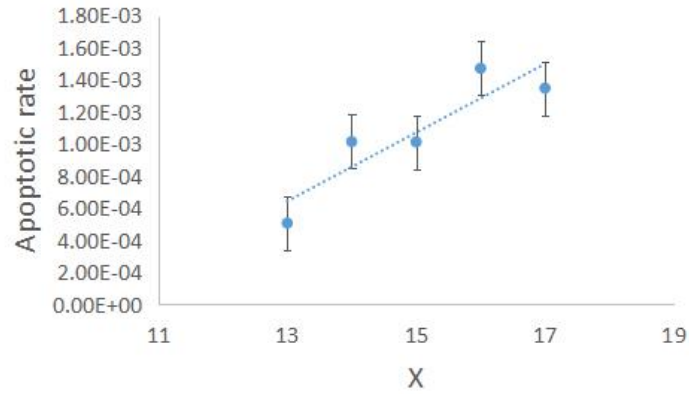


Figure 8: The positive correlation between the tumorous cells' apoptotic rate and the parameter  $X$ , which controls cells' contractility.

### 3.6 The simulation results does not fit well with the mathematical model in terms of the critical size of the initial tumor.

The simulation results show a poor agreement with our mathematical model's prediction. According to the mathematical model, the critical size  $z_c$  represents the critical radius of the tumor, which leads to the critical tumor area to be  $A_c = \pi z_c^2$ . Accordingly, the critical tumorous cells number should be

$$N_c = \frac{A_c}{\pi \langle r \rangle^2} = \frac{\pi \tilde{z}_c^2 \langle r \rangle^2}{\pi \langle r \rangle^2} = \tilde{z}_c^2. \text{ Moreover, based on the mathematical model } z_c = 4 \left( 1 + \frac{\gamma}{\mu} \right), \text{ where}$$

$\gamma$  stands for apoptotic rate and equals to  $\gamma = 1 \times 10^{-3}$  in our simulation, and  $\mu$  accounts for proliferation rate and gets the value  $\mu = 4 \times 10^{-5}$ , leading to  $\tilde{z}_c = 104$  and  $N_c = 10^4$ . The critical number of tumorous cells estimated from the mathematical model shows a bad fit with our simulation result, which may be caused by the overestimated value of the parameter  $X$ , leading to an unfair apoptotic rate of tumorous cells. Besides, there may be other functions rather than a linear function that can better describe the death cells numbers change over time.

#### 4. Discussion:

Overall, our study shows an evidence that *scrib*-defective mutant cells are able to proliferate indefinitely, but are always eliminated by cell competition when interact with normal tissue. Despite of their overgrowth capability, we show that oncogenic *scrib*<sup>-</sup> cells of the growing tumor are killed by *JNK*-mediated apoptosis when surrounded by wild-type cells. It implies that maybe we could kill the tumor through actively inducing the production of *JNK* via certain stimulation to cause mutation of *JNK* to trigger the apoptosis of tumorous cells, which may be a leading research filed for the cancer treatment in the future.

The microenvironment hypothesis predicts that the progression of a *scrib*<sup>-</sup> tumor requires the formation of a protective microenvironment with sufficient cell density to allow the inside cells to evade cell competition. It has been reported that small-size tumor patches merging could rescue the tumor from being eliminated by cell competition. We show strong support for the hypothesis here with the simulation observations that the tumor can overcome the apoptosis pressure exerted by the surrounding wild-type tissue and expand, with a large enough initial size ( around 121 tumorous cells). Even though it shows a poor matching with the mathematical model prediction, our result shows evidence that there does exist a critical size that determines tumors' fate. This finding could mean a novel treatment method for clearing tumors in the near future via breaking down large-size tumors into several small parts, which may take the advantage of cell competition to eliminate the tumor groups, since the small tumor patches cannot overcome the apoptotic pressure exerted from the surrounding normal tissue and are going to be cleared out from the tissue.

Moreover, it has been reported that apoptotic cells can secrete proliferative signals, which may act as a tumor stimulation mechanism of cell competition in tumor progression. It has been argued that the *JNK* pathway is mainly responsible for inducing the survival signal *Dpp* and *Wg*, which generates a compensatory proliferation to promote tumor growth.<sup>20,23</sup> Accordingly, simulations can be run to induce the production of *Dpp* by *JNK* signals from the apoptosis zone and promote the proliferation of the cells that localized close to the dead cells via forming a gradient of the *Dpp* concentration. However, it is still unclear why apoptosis activity of cells occurs close to the zone with high *Dpp* signals. Also, what we still do not understand is that both mutant cells and wild-type cells that located close to the dead cells have the same opportunity to capture the *Dpp* signals, which means both types of cells have the chance to enhance their proliferation rate, but why exactly this process promotes tumors' growth in the end and makes tumors win the cell competition. A ligand capture model has been proposed, which suggests that the ability of capturing morphogen signals may be different among different cell types, leading to the *JNK*-mediated apoptosis of the cells with low morphogen signals.<sup>1,8</sup> However, the specific mechanism involved in morphogen promoting tumor progression is still unknown and it may be a significant breakthrough for cancer treatment in the future if we could stop morphogen promoting tumors' growth, maybe via inducing a mutation of the ligands' receptor if the ligand capturing model is true.

Overall, cell competition could be a significantly prospective research field for the innovation of the tumor treatment methods in the future, either from the point of *JNK*-mediated apoptosis, or *Dpp* induced compensatory proliferation, as well as the merging behavior of the tumor to form a protective microenvironment. There are still many mystery concerning about the role of cell competition in tumor progression, that need to be explored, but hopefully we can finally beat the tumor via intensifying cell

competition one day in the very near future.

## References

1. Amoyel M. and Bach E.A. (2014). Cell competition: how to eliminate your neighbours. *The company of Biologists* 141, 988-1000.
2. Anna Kicheva, Periklis Pantazis, Tobias Bollenbach, Yannis Kalaidzidis, Thomas Bittig, Frank Jülicher, Marcos González-Gaitán. (2007). *Science* 315, 521-525.
3. Brumby A.M. (2003). Scribble (Scrib) mutants cooperates with oncogenic Ras and Notch to cause Neoplastic overgrowth in *Drosophila*. *EMBO* 22(21), 5769 – 5779.
4. Buceta J. and Canela-Xandri O. (2014). TiFoSi: an Efficient Simulation Suite for Epithelia. In preparation.
5. Canela-Xandri O., Sagues F., Cassdemunt J., and Buceta J. (2011). Dynamics and Mechanical Stability of the Developing Dorsoventral Organizer of the Wing Imaginal Disc. *PLoS Computational Biology* 7, e1002153.
6. Chiao-Lin Chen, Molly C. Schroeder, Madhuri Kango-Singh, Chunyao Tao and Georg Halder. (2011). Tumor suppression by cell competition through regulation of the Hippo pathway. *PNAS* 109, 484-489.
7. Claveria C.L., Giovinazzo, G., Sierra, R. and Torres M. (2013). Myc-driven endogenous cell competition in the early mammalian embryo. *Nature* 500,39-44.
8. Eduardo M. (2008). Is cell competition relevant to cancer? *Nature* 8, 141-146.
9. Farhadifar R., Roper J.C., Aigouy B., Eaton S., and Julicher F. (2007). The influence of Cell Mechanics, Cell-cell Interactions, and Proliferation on Epithelial Packing. *Current Biology* 17, 2095-2104.
10. Fei Chen. (2012). JNK-Induced Apoptosis, Compensatory Growth, and Cancer Stem Cells. *Cancer Research* 72, 379-387.
11. Floris Bosveld, Boris Guirao, Zhimin Wang, Mathieu Rivière, Isabelle Bonnet, Francois Graner and Yohanns Bellaïche. (2016). Modulation of junction tension by tumor suppressors and protooncogenes regulates cell-cell contacts. *The Company of Biologists Ltd* 143, 623-634.
12. Francesca Froidi, Marcello Ziosi, Flavio Garoia, Andrea Pession, Nicola A Grzeschik, Paola Bellosta, Dennis Strand, Helena E Richardson, Annalisa Pession and Daniela Grifoni. (2010). The lethal giant larvae tumour suppressor mutation requires dMyc oncoprotein to promote clonal malignancy. *BMC Biology*, <http://www.biomedcentral.com/1741-7007/8/33>.
13. Gines Morata and Luna Ballesteros-Arias. (2015). Cell competition, apoptosis and tumour development. *Int.J.Dev.Biol.*59, 79-86.

14. Hisao Honda, Masaharu Tanemura and Tatsuzo Nagaic. (2003). A three-dimensional vertex dynamics cell model of space-filling polyhedra simulating cell behavior in a cell aggregate. *Theoretical Biology* 226, 439-453.
15. Hyung Don Ryoo, Travis Gorenc, and Hermann Steller. (2004). Apoptotic Cells Can Induce Compensatory Cell Proliferation through the JNK and the Wingless Signaling Pathways. *Developmental Cell*, Vol. 7, 491 – 501.
16. Igor Sokolov. (2007). Atomic Force Microscopy in Cancer Cell Research. *Cancer Nanotechnology*, 1-17.
17. Javier Buceta. (2016). Neoplastic Tumor Progression. *Notes*.
18. J. Buceta and O. Canela-Xandri. (2014). TiFoSi: an Efficient Simulation Suit for Epithelia.
19. Javier Menéndez, Ainhoa Perez-Garijo, Manuel Calleja and Gines Morata. (2010). A tumor-suppressing mechanism in *Drosophila* involving cell competition and the Hippo pathway. *PNAS* 107, 14651-14656.
20. John M. Abrams. (2002). Competition and Compensation: Coupled to Death in Development and Cancer. *Cell* 110, 403-406.
21. Johnston L.A., Prober D.A., Edgar, B.A., Eisenman R.N. and Gallant P. (1999). *Drosophila* Myc regulates cellular growth during development. *Cell* 98, 779-790.
22. Jun R. Huh1, Ming Guo2, and Bruce A. Hay. (2004). Compensatory Proliferation Induced by Cell Death in the *Drosophila* Wing Disc Requires Activity of the Apical Cell Death Caspase Dronc in a Nonapoptotic Role. *Current Biology* 14, 1262 – 1266.
23. L Ballesteros-Arias, V Saavedra and G Morata. (2013). Cell competition may function a tumour-suppressing or as tumour-stimulating factor in *Drosophila*. *Oncogene* 33, 4377-4384.
24. Manuel Théry, Michel Bornens. (2006). Cell shape and cell division. *Current Opinion in Cell Biology*. Volume 18, Issue 6, 648-657.
25. Mark Norman, Katarzyna A. Wisniewska, Kate Lawrenson, Pablo Garcia-Miranda, Masazumi Tada, Mihoko Kajita, Hiroki Mano, Susumu Ishikawa, Masaya Ikegawa, Takashi Shimada, Yasuyuki Fujita. (2012). Loss of Scribble causes cell competition in mammalian cells. *Cell Science* 125, 59-66.
26. Menendez J., Perez-Garijo A., Calleja M. and Morata G. (2010). A tumor-suppressing mechanism in *Drosophila* involving cell competition and the Hippo pathway. *Proc.Natl.Acad.Sci.USA* 107, 14651-14656.
27. M. Lekka, P. Laidler, D. Gil, J. Lekki, Z. Stachura and A.Z. Hryniewicz. (1999). Elasticity of normal and cancerous human bladder cells studied by scanning force microscopy. *Eur Biophys J* 28, 312-316.
28. Nicholas E. Baker and Wei Li. (2008). Cell Competition and Its Possible Relation to Cancer. *Cancer Ras* 68, 5505-5507.

29.Simon Tanaka. (2015). Simulation Frameworks for Morphogenetic Problems. *Computation* 3, 197-221.

30.Simpson P. (1979). Parameters of cell competition of the wing disc of *Drosophila*, *Dev.Biol.*69,182-193.

31.Simpson P. and Morata,G. (1981). Differential mitotic rates and patterns of growth in compartments in the *Drosophila* wing.*Dev.Biol.*85,299-308.

32.Teresa Eichenlaub, Stephen M. Cohen and Hector Herranz. (2016). Cell Competition Drives the Formation of Metastasis Tumors in a *Drosophila* Model of Epithelial Tumor Formation. *Current Biology* 26,1-9.



**Vita:**

Bixi Kang

Born in 1992, In China

2011 graduated from Nanjing Normal  
University with a bachelor's degree from  
Biotechnology major

Father's name: Sen Kang

Mother's name: Ling Wang